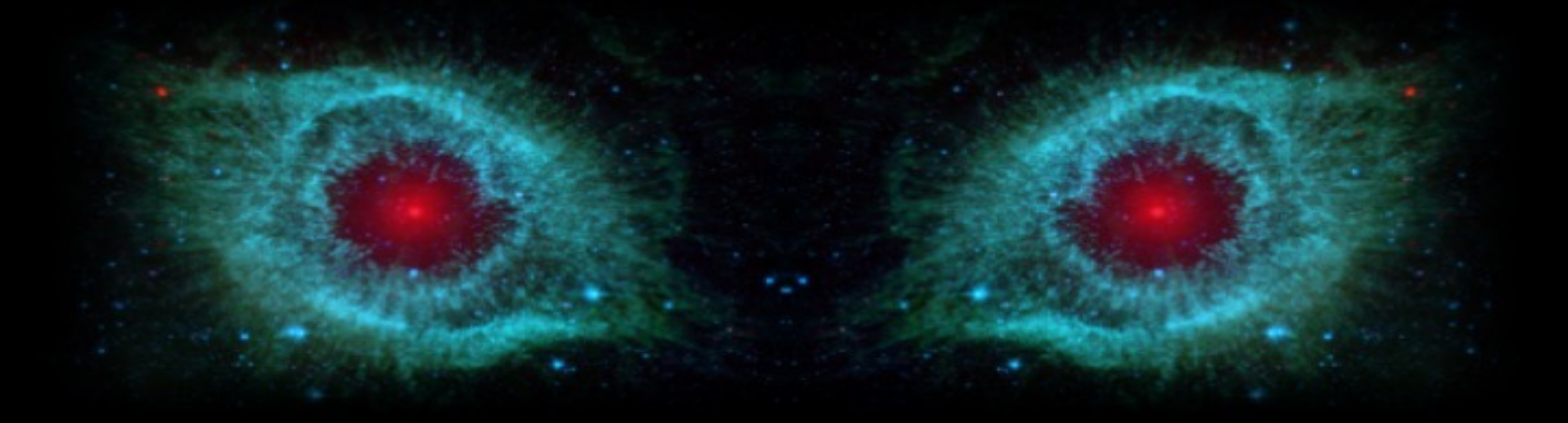

LSW experiments in the microwaves

Istituto Nazionale di Fisica Nucleare

16TH PATRAS WORKSHOP

June 15, 2021

Paolo SPAGNOLO

INFN – Pisa - Italy

Outline

- Experimental overview
- LSW experimental scheme
- MW experiment design
- Magnets, detectors and cavities
- MW potential in the experimental landscape
- Conclusions

Axions Experiments

3 classes of experiments: Haloscopic, Helioscopic, Laboratory (LSW)

Axion, like neutral pion couples to
two photons via Primakoff effect)
Detected in a magnetic field H

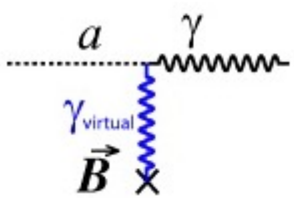

$m_a < 3\text{x}10^{-3}$ eV from SN1987

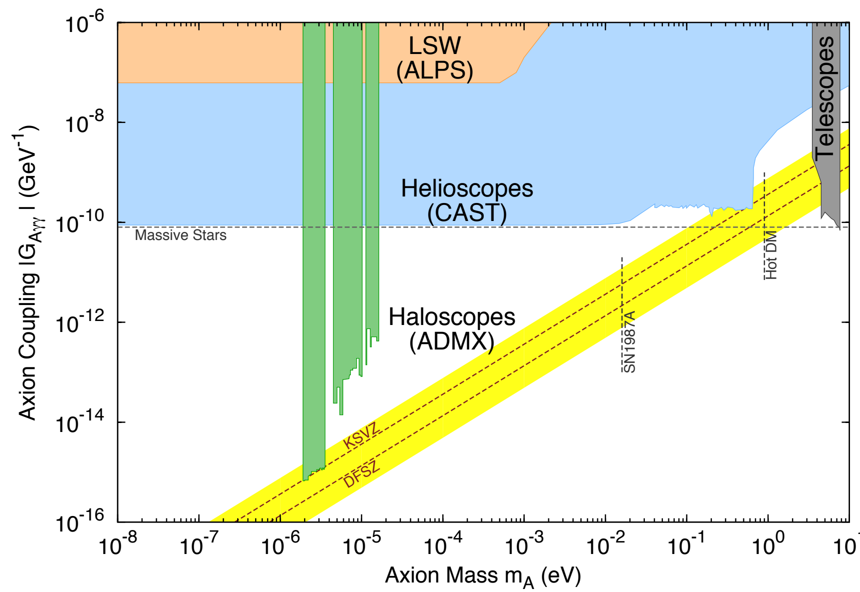

Yellow band represent theoretical predictions from DFSZ and KSVZ axion models

Haloscopic: cavity like ADMX

Are the only experiments hitting the Peccei-Quin region

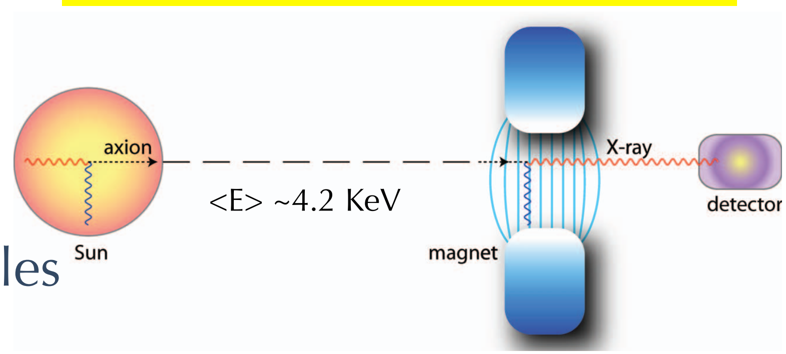

Helioscopic: depend on stellar models

CAST (best limit at the moment) withLHC dipoles

IAXO (next Helio. exp.)

Light Shining through a Wall Experiments

P. Sikivie, Phys. Rev. Lett. **51**, 1415 (1983)

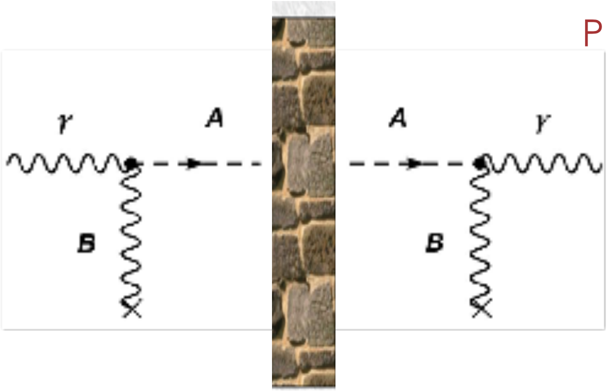

LAB experiment
Laser Source
Higher Luminosity

Double process
Rate ~ G^4

$$\dot{N}_{\text{evts}} \propto \dot{N}_\gamma \, P_{\gamma\to a} \times P_{a\to\gamma} \sim \dot{N}_\gamma \, G^4 H^4 L^4$$

Sensitivity on G linear with L and H, quartic root of luminosity (not depending on E_γ)

10^{19} photons hitting the wall

1 single photon beyond the wall

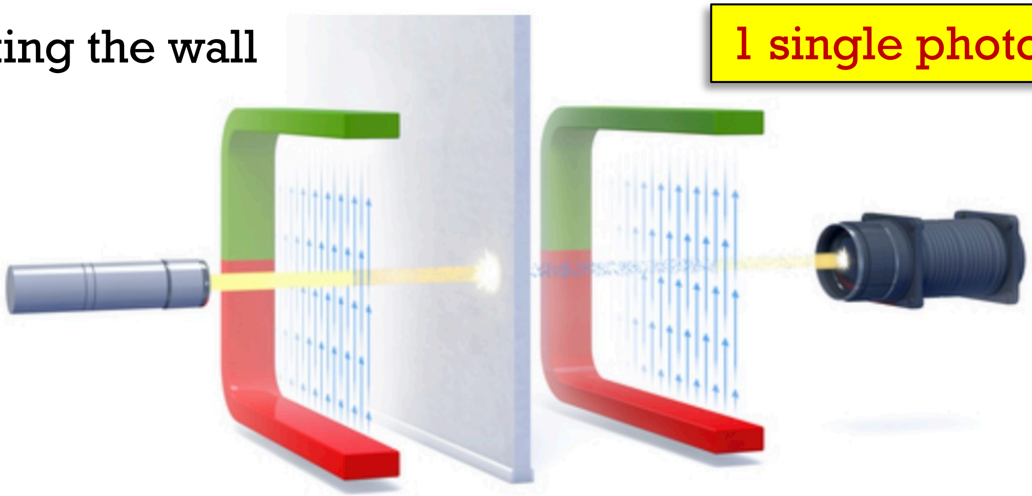

+ Phys. Dark Univ. **12**, 37 (2016)

Physics of the Dark Universe 12 (2016) 37–44

ELSEVIER

Contents lists available at ScienceDirect

Physics of the Dark Universe

journal homepage: www.elsevier.com/locate/dark

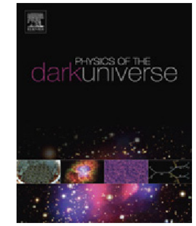

Axion-like particle searches with sub-THz photons

CrossMark

L.M. Capparelli [a], G. Cavoto [b], J. Ferretti [c], F. Giazotto [d], A.D. Polosa [c,e,∗], P. Spagnolo [f]

[a] *Department of Physics and Astronomy, University of California Los Angeles, 475 Portola Plaza, Los Angeles, CA 90095, USA*
[b] *INFN Sezione di Roma, P.le Aldo Moro 5, I-00185 Roma, Italy*
[c] *Dipartimento di Fisica and INFN, 'Sapienza' Università di Roma, P.le Aldo Moro 5, I-00185 Roma, Italy*
[d] *NEST, Istituto Nanoscienze-CNR and Scuola Normale Superiore, I-56127 Pisa, Italy*
[e] *CERN-TH, CH-1211 Geneva 23, Switzerland*
[f] *INFN Sezione di Pisa, Largo Bruno Pontecorvo, 3, 56127 Pisa, Italy*

A R T I C L E I N F O

Article history:
Received 23 October 2015
Received in revised form
28 January 2016
Accepted 29 January 2016

Keywords:
Axion-like particles
Dark-matter constituents
Paraphotons
Chameleons
Light-Shining-through-Wall experiments

A B S T R A C T

We propose a variation, based on very low energy and extremely intense photon sources, on the well established technique of Light-Shining-through-Wall (LSW) experiments for axion-like particle searches. With radiation sources at 30 GHz, we compute that present laboratory exclusion limits on axion-like particles might be improved by at least four orders of magnitude, for masses $m_a \lesssim 0.01$ meV. This could motivate research and development programs on dedicated single-photon sub-THz detectors.

Presented at ICHEP16

Optimization attempt of LSW scheme

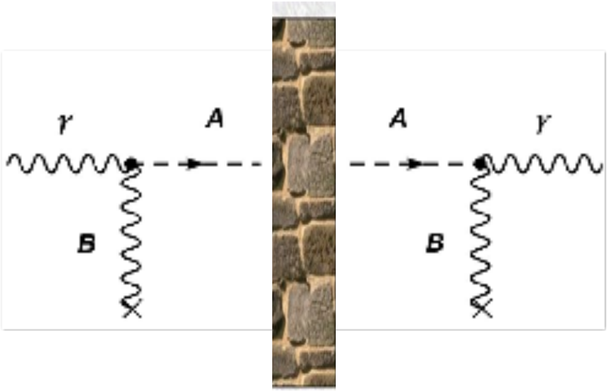

Gyro-Klystrom Source
Highest Luminosity

$$\dot{N}_{\text{evts}} \propto \dot{N}_\gamma \, P_{\gamma\to a} \times P_{a\to\gamma} \sim \dot{N}_\gamma \, G^4 H^4 L^4$$

Sensitivity on G linear with L and H, quartic root of luminosity (not depending on E_γ)

The key points are:

- High Luminosity (gyrotrons in the SubTHz region)
- intense H ~ 11 Tesla with L ~ 150 cm dipole
- Sub-THz **single photon** detector using TES

Optimal Working Point ~ **30-100 GHz** (microwaves)

High Luminosity Photon Sources

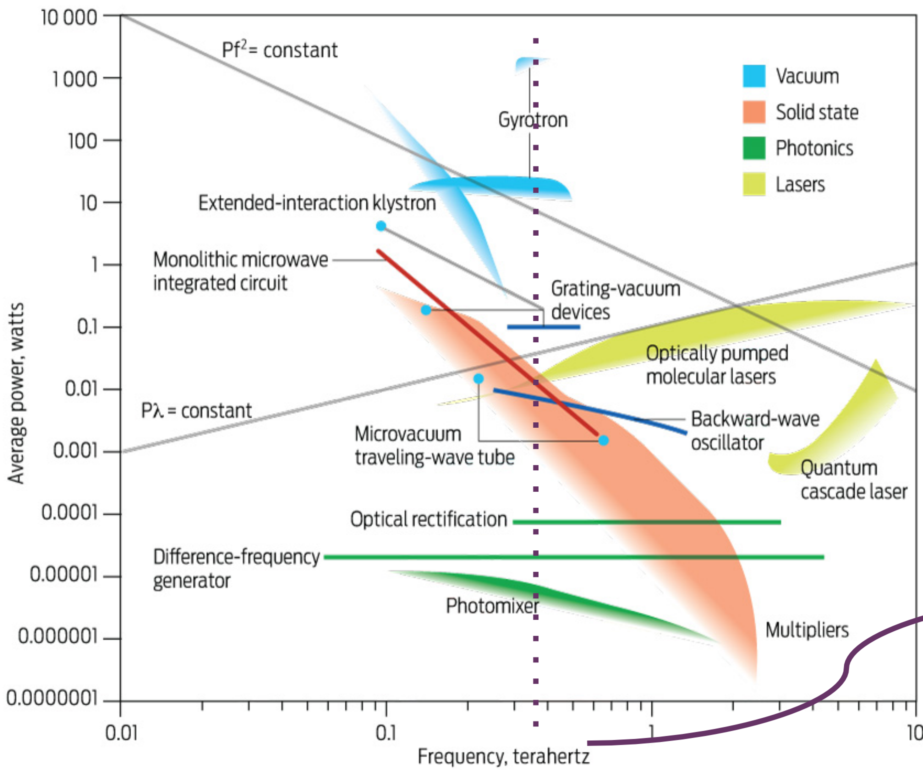

photon-axion conversion probability depends on luminosity, not energy

$\Rightarrow$ Lumi = P(ω)/E(ω)

Reference:

30 GHz ~ 120 μeV ~ 1 cm

Micro-waves domain

- Klystrons and gyrotrons sources in the 30-100 GHz range.
- Power exceeding 1 MW in this frequency range
- Luminosity up to 10^{28}-10^{29} γ/s in CW
- Lasers commonly used in LSW experiments ~ 10^{19} γ/s

High Luminosity Photon Sources

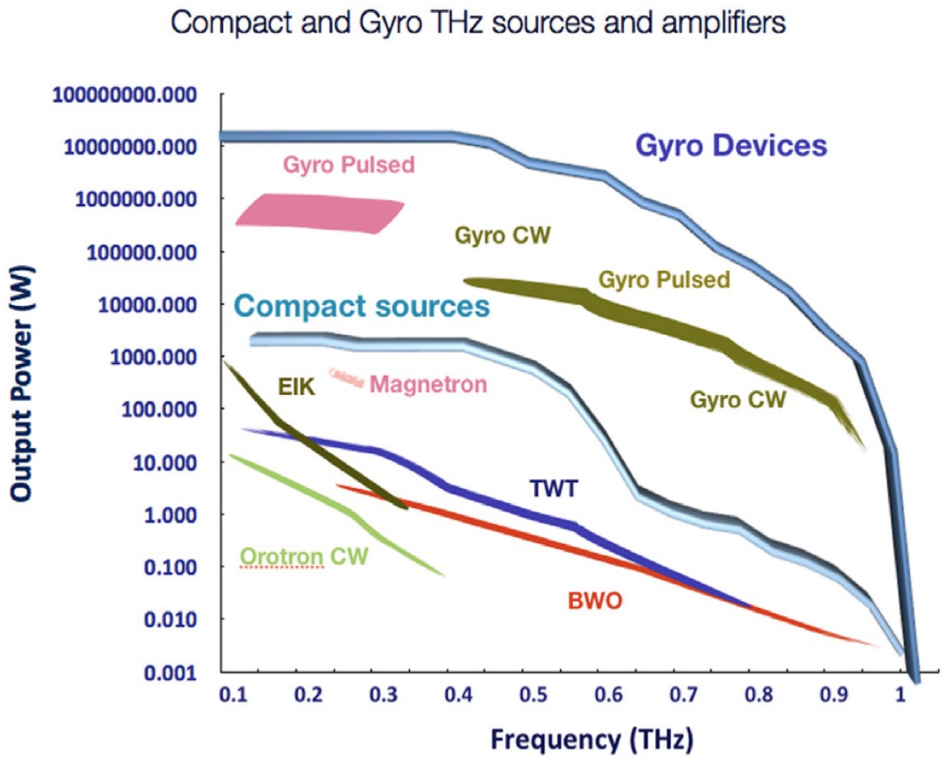

photon-axion conversion probability depends on luminosity, not energy

$\Rightarrow$ Lumi = $P(\omega)/E(\omega)$

Reference:
30 GHz ~ 120 μeV ~ 1 cm
Micro-waves domain

- Klystrons and gyrotrons sources in the 30-100 GHz range.
- **Power exceeding 1 MW** in this frequency range
- Luminosity up to 10^{28}-10^{29} γ/s in CW
- Lasers commonly used in LSW experiments up to 10^{19} γ/s

Micro-Wave Experimental scheme

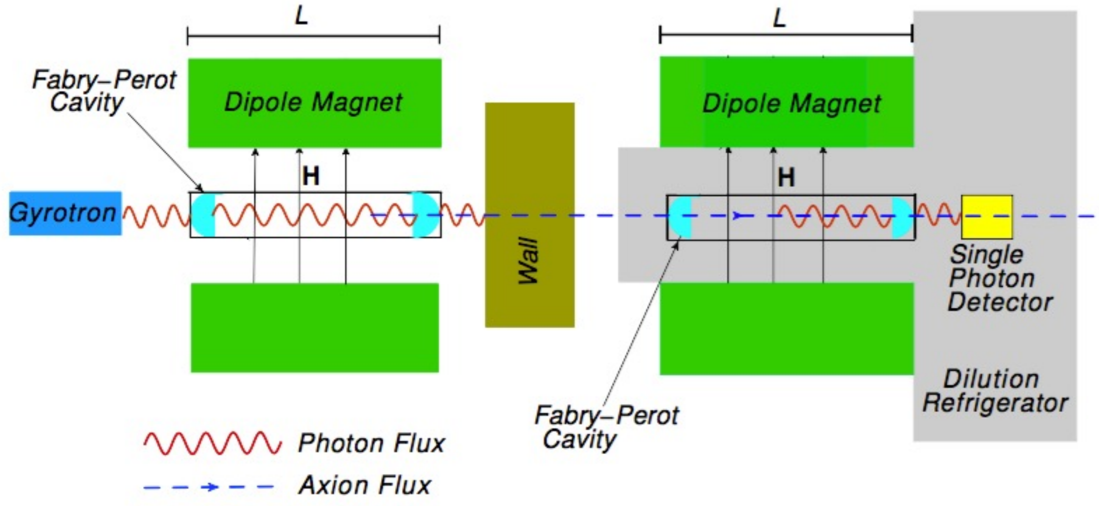

- Magnetic field: $H = 11$ T, $L = 1.5$ m
- Source: gyrotron; $P \approx 100$ kW, $\Phi_\gamma = 10^{27}$ s^{-1}, $\varepsilon_\gamma = 120$ μeV ($\nu \approx 30$ GHz)
- Fabry-Perot cavity: finesse $Q \approx 10^4$

- Sub-THz single-photon detection based on TES technology, $\eta \approx 1$
- Possible second FP cavity behind the wall to enhance axion-photon conversion rate

P. Sikivie, D.B. Tanner and K. Van Bibber, Phys. Rev. Lett. 98, 172002 (2007)

11T CERN dipole magnets

- The HL-LHC Project implies beams of larger intensity
  - Additional collimators are needed
- Two collimators to be installed on either side of interaction point 7
  - Replace a standard Main Dipole by a pair of shorter 11 T Dipoles
- 5 single aperture short models fabricated and tested by CERN TE-MSC team
  - Bore field ranging from 10 to 12 T
  - 60 mm coil aperture
  - ~1.5 m magnetic length

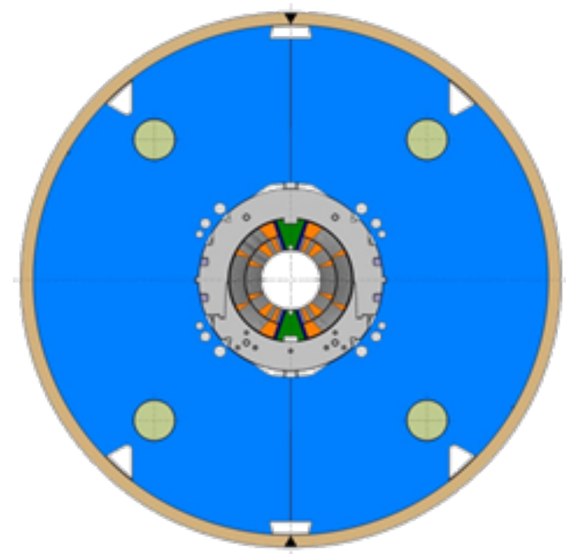

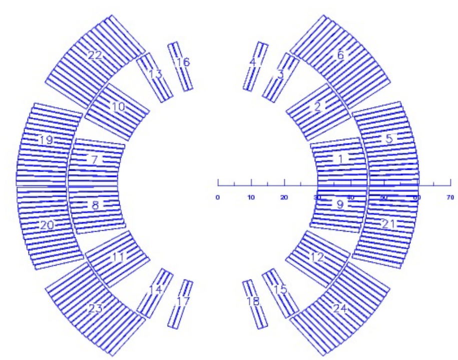

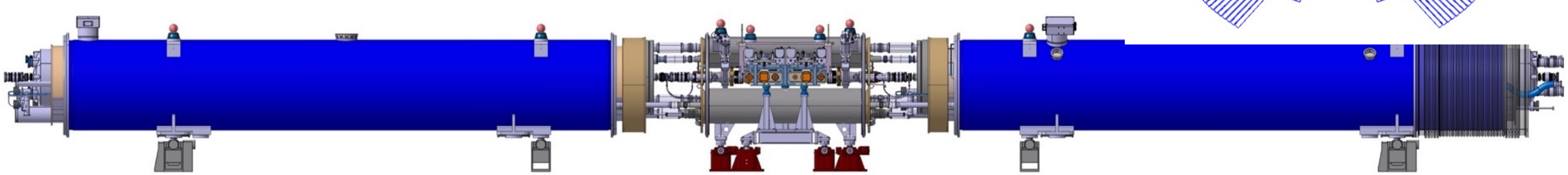

Included in the PBC CERN document for EU strategy

11T CERN dipole magnets

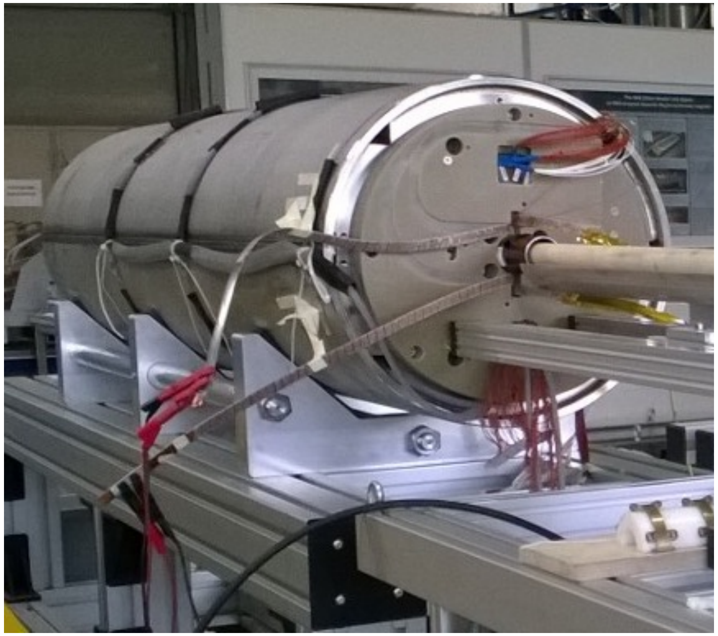

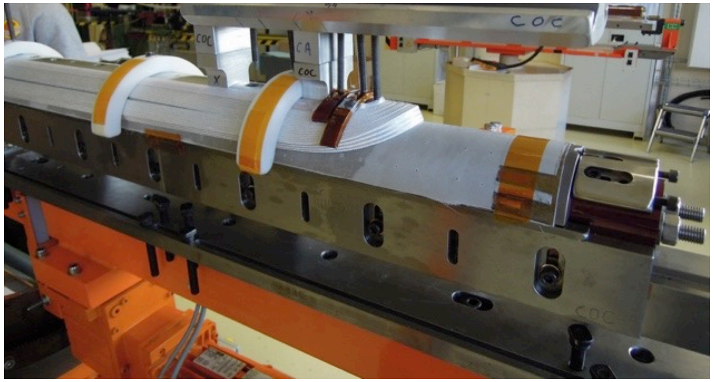

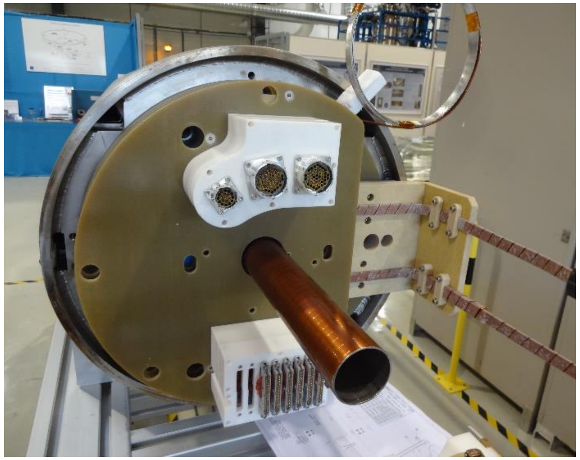

Berkley - CCT6 and TFD

- **C**anted **C**os-**T**heta CCT6
  - Goal: Nb_3Sn magnet for testing HTS coils
  - Round aperture with 120 mm diameter
  - Target field: 12 T at 4.2 K over 200 mm length
  - Design in progress; fabrication at LBNL expected in 2022-2023
  - Funded by DoE HEP as part of the LBNL Magnet Development Program

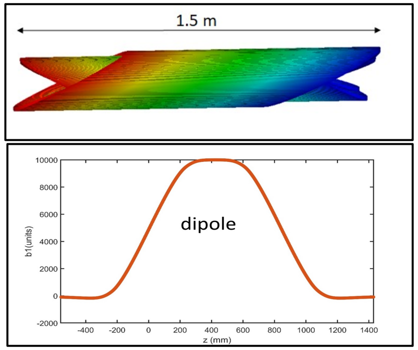

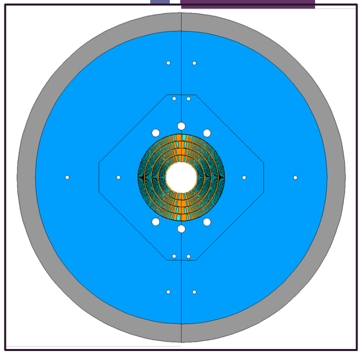

- **T**est **F**acility **D**ipole TDF
  - Goal: Nb_3Sn magnet for testing superconducting cables
  - Rectangular aperture: 150x100 mm diameter
  - Target field: 14-15 T at 4.2 K over ~800 mm length
  - Design in progress; fabrication at LBNL expected in 2022-2024
  - Funded by DoE HEP and FES (Fusion Energy Science)

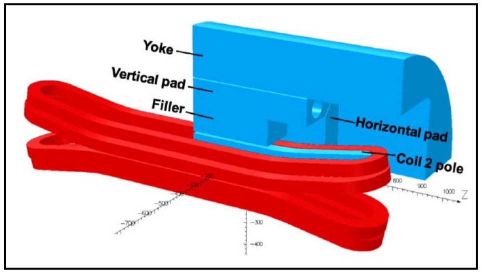

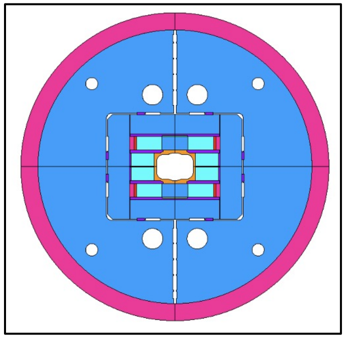

Transition Edge Sensor

TES operates within its superconducting transition. DC bias voltage applied.
When TES absorbs an incoming photon, it heats up above critical temperature Tc.
Change of resistance and current flowing in the circuit, measured by a SQUID

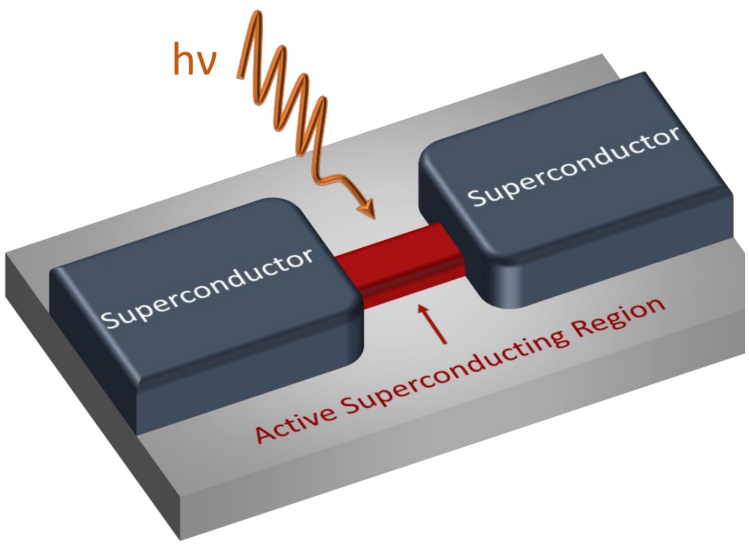

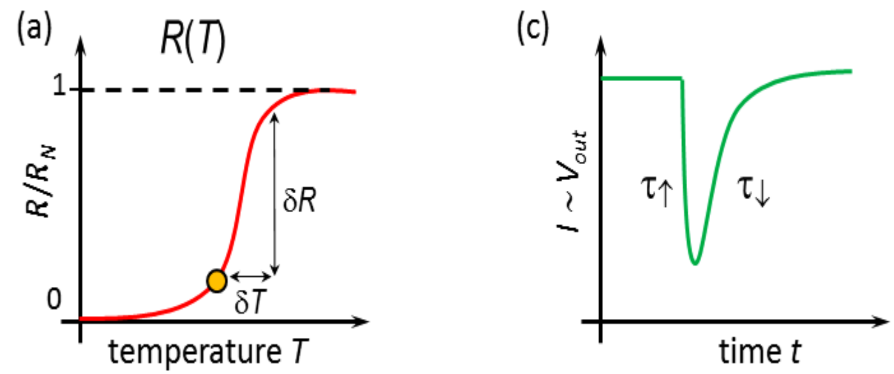

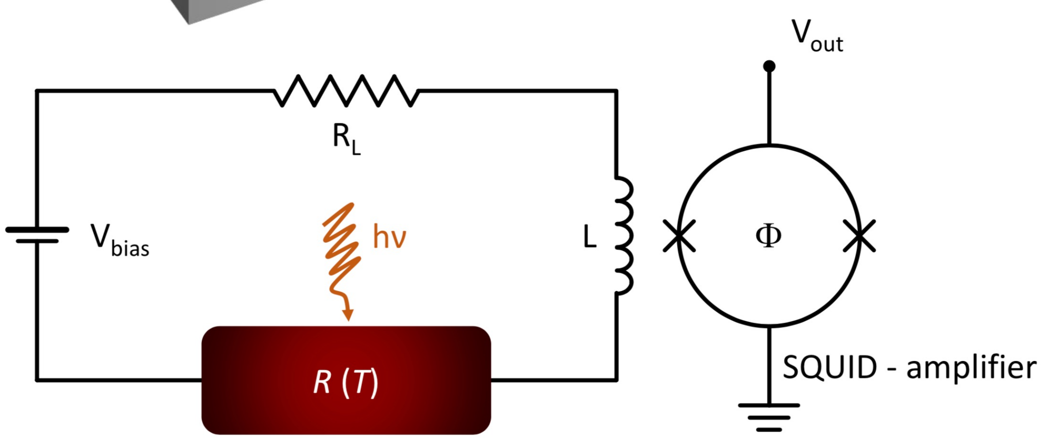

Figure of merit: $\alpha = \frac{T}{R}\frac{dR}{dT}$

R - resistance of active region
T - temperature of active region

Energy resolution: $\Delta E \cong 2.35\sqrt{2k_B T^2 \frac{C}{\alpha}}$
k_B - Boltzmann constant
Heat capacity: $C = \gamma V_{Active} T$
γ - Sommerfeld coefficient
V_{Active} - active region volume

Transition Edge Sensor

TES operates within its superconducting transition. DC bias voltage applied.
When TES absorbs an incoming photon, it heats up above critical temperature Tc.
Change of resistance and current flowing in the circuit, measured by a SQUID

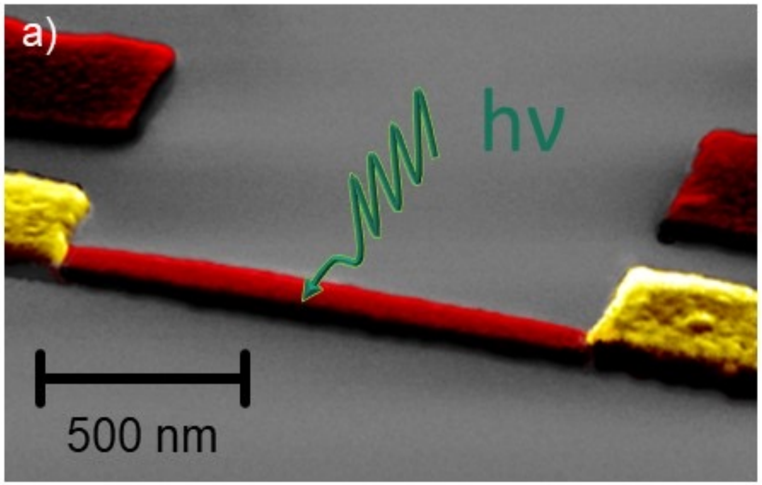

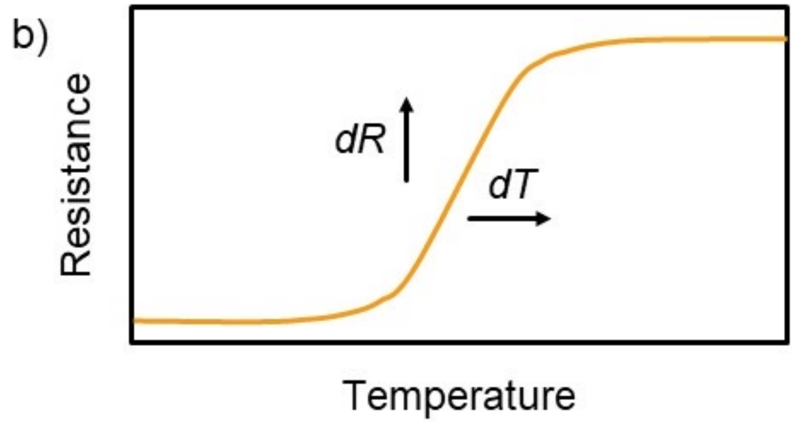

Active region
Lateral electrodes

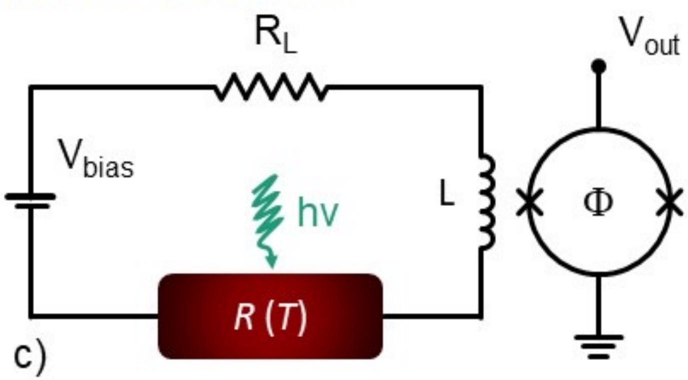

Electro-thermal parameter $\alpha = \frac{T}{R}\frac{dR}{dT}$

R - resistance of active region
T - temperature of active region

Energy resolution: $\Delta E \cong 2.35\sqrt{2k_B T^2 \frac{C}{\alpha}}$
k_B - Boltzmann constant
Heat capacity: $C = \gamma V_{Active} T$
γ - Sommerfeld coefficient
V_{Active} - active region volume

d)

TES detectors

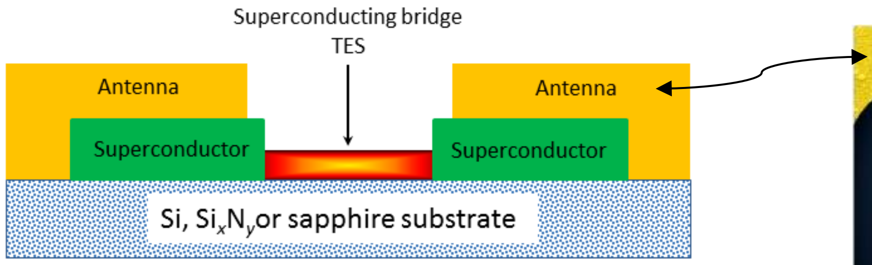

- Sub-THz single photon detector
- Transition Edge Sensor TES: ultra-low critical temperature superconductor bridge between two superconducting electrodes. TES coupled to a log periodic antenna.
- Goal: Energy resolution below 10%
- Tailoring active volume to reduce thermal capacitance ($V \sim 300 \times 40 \times 20$ nm $^3 < 10^{-3} \mu m^3$)
  Material: choice of a Superconductor with low critical temperature ($T_c \approx 30$ - 50 mK) to have a good energy resolution bilayer Ti-Au, Al-Cu or Ti-Cu
- TES bridge Ti-Cu (gap ~20 μeV), superconducting electrodes Nb (gap ~ 1 meV)
- Very high efficiency
- Ultra low background/dark count

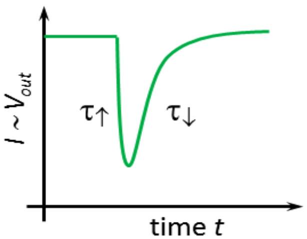

Transition Edge Sensors: Critical Temperature

For axions detection: $T_{C,Active}$~20mK

Phys. Dark Universe **12**, 37 (2016)

T_C suppression by spatial confinement

Phys. Rev. B **85**, 094508 (2012)C

T_C suppression by vertical inverse proximity effect

Superconductivity Of Metals And Alloys, Advanced Books Classics (Westview Press, 1999)

Reduction of the wire section:
constant thickness *t*
smaller width *W*

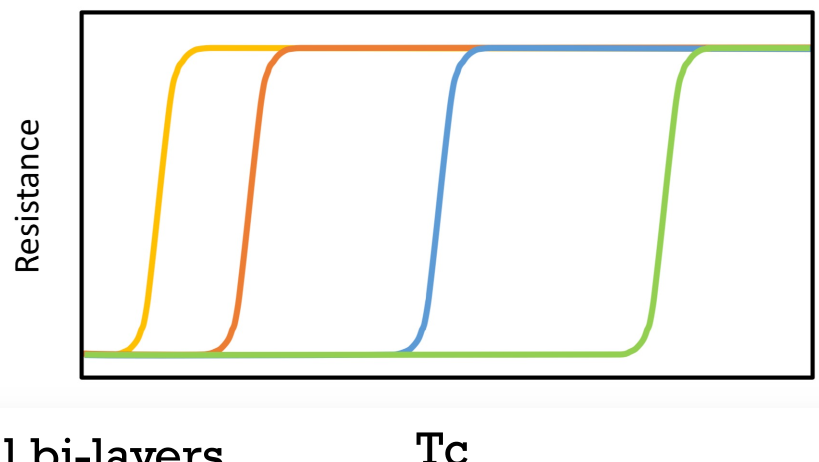

Bilayer:
Normal metal
Superconductor

Cu-Al bi-layers

Tc dependence by spatial confinement

Ti nanowires

Reduction of the wire section:
constant thickness *t*
smaller width *W*

Phys. Rev. B **85**, 094508 (2012)

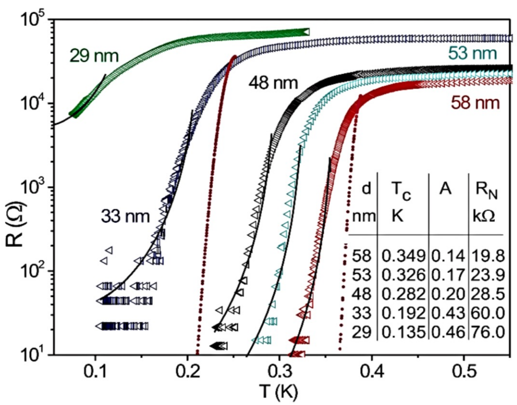

The *Tc* decreases with the decrease of nanowire cross-section

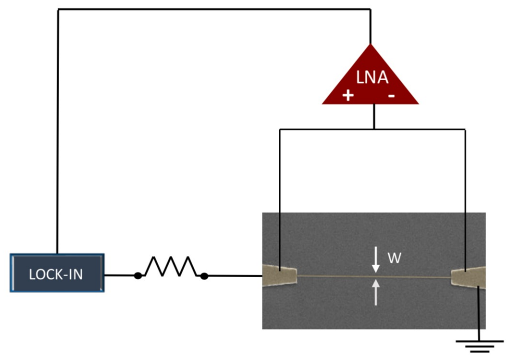

Width **W** (nm)	**Thickness** **t** (nm)	**Tc** (mK)
200	30	540
60	30	210

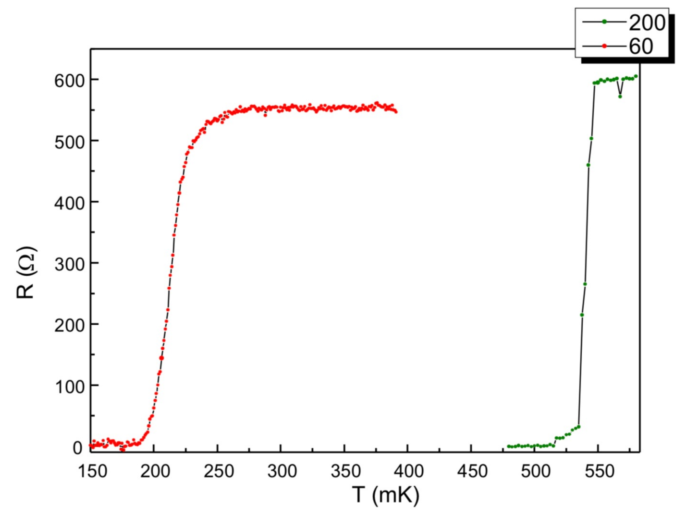

Tc suppression by vertical inverse proximity effect

Reduction of the wire section:
constant width *W*
smaller thickness *t*

Cu/Al bilayer

t_N: thickness Cu
t_S: thickness Al

	A	B	C
W (nm)	120	120	120
Cu Thickness (nm)	14	15	15.5
Al Thickness (nm)	10	10	10

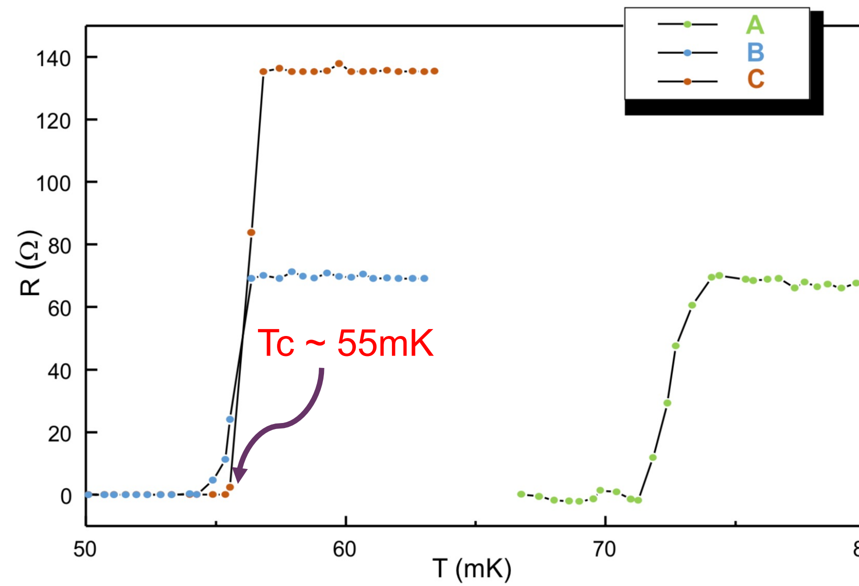

Low control on grain size for thin-film deposited at room temperature

Generation and the Regeneration Cavities

Finesse of about 10^4 is expected
A classic Fabry Perot, in the range 30-100 GHz could bring to the beam confinement problem

The waist of the photon beam should be of few cm in order to have a total cavity length of 1.5 m to be fully inserted into the dipole magnet

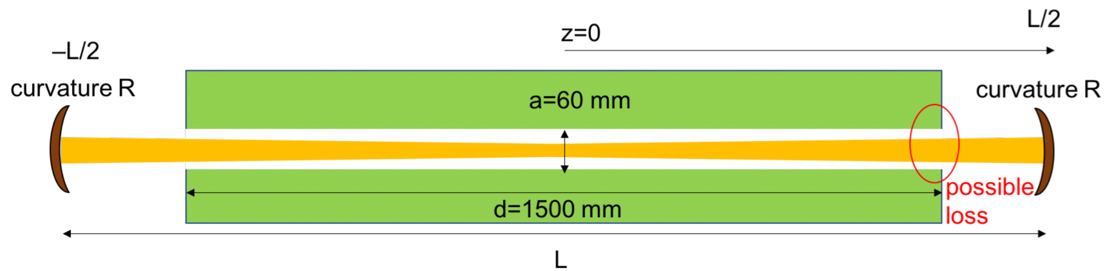

A valid alternative could be a corrugated waveguide structure to confine millimetre waves in a linearly polarized HE11 mode

In high power applications it minimizes the power loss at the waveguide wall
Need to investigate a set of materials suitable for application in high magnetic fields

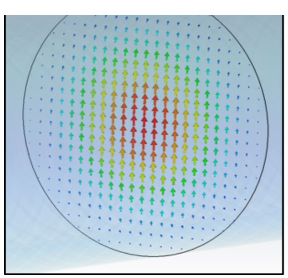

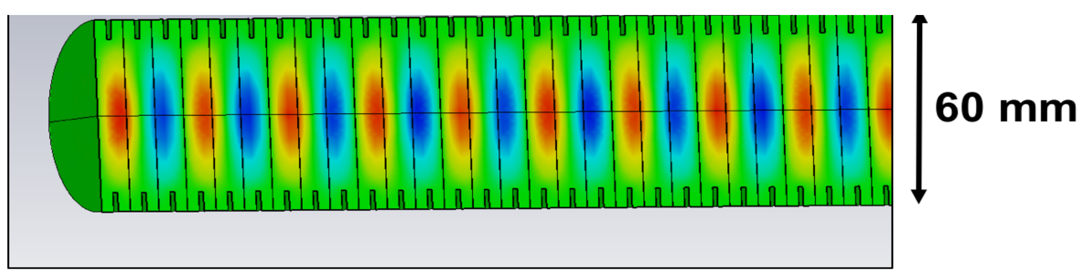

Courtesy of Akira Myazaki (his talk later today)

Next Steps…

- Cu/Ti down to Tc ~ 20-30 mK (via a cold deposition)
- Coupling with a SQUID read-out
- Test with a 30-100 GHz photon source
- R&D of the Fabry Perot
- Design of the log periodic antenna

Alternative choices to boost the experiment

- Work with a new concept Fabry Perot after the wall to enhance the finesse Q
- An upgrade in Q translates into the need of a lower power of the source P/Q^2

$$\dot{N}_{\text{evts}} \propto \dot{N}_\gamma \, P_{\gamma\to a} \times P_{a\to\gamma} \ \text{x QxQ}'$$

- Fabry Perot with Q′ exceeding 10^{10} have been recently developed with superconducting cavities or *wispering galleries resonator*

- Material choice need to be shaped to work in this particular environment
  - Low temp
  - High B field
- High Q and lower P can drive the use of other (more refined and easier to handle) photon sources than gyrotrons (klystrons?)

Constraints on $g_{A\gamma\gamma}$ vs. m_A

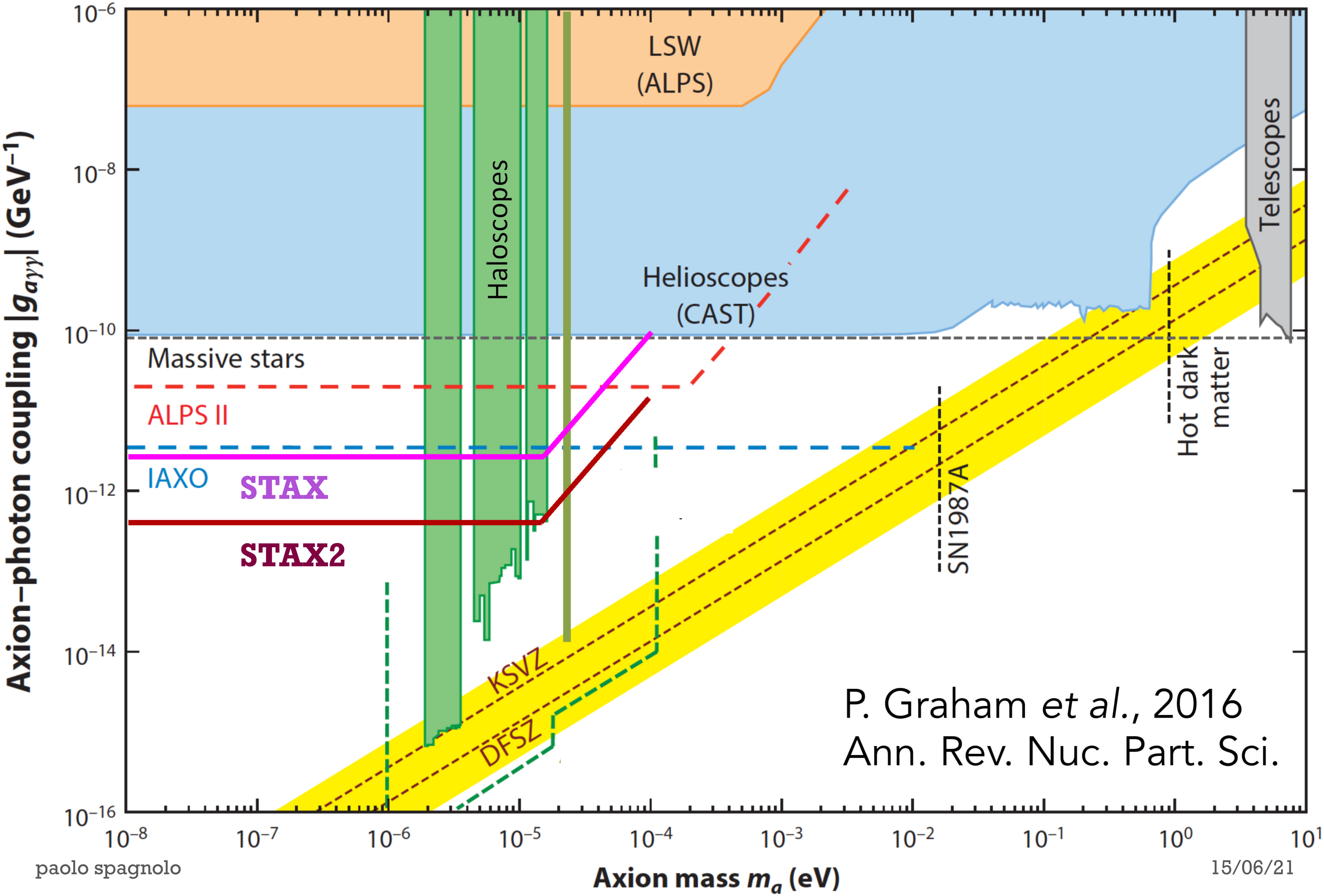

CONCLUSIONS

- A new optimized version of the LSW experiments is proposed
- The ambitious goal is to push limit on the *photon-axion* coupling ***g*** beyond stellar experiments (CAST) exclusion
- Development of Fabry-Perot and TES detectors could lead to a new generation of experiments in the field
- Important R&D need to be addressed to the scope

Nanotech detectors could drive Searches of Light Dark Matter

BACK UP SLIDES

Josephson Escape Sensor (JES)

J. Appl. Phys. **128**, 194502 (2020);
https://doi.org/10.1063/5.0021996

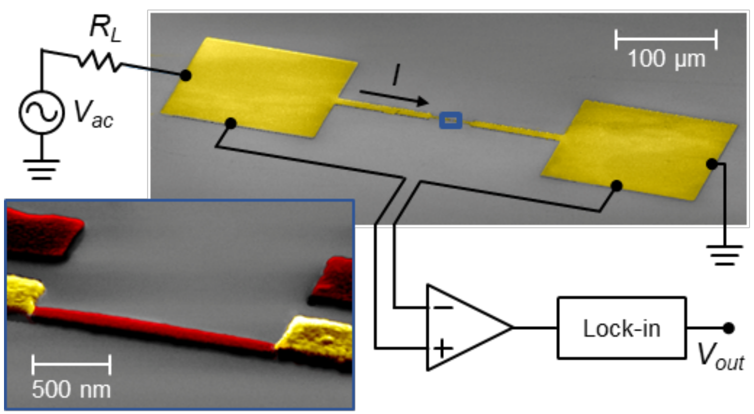

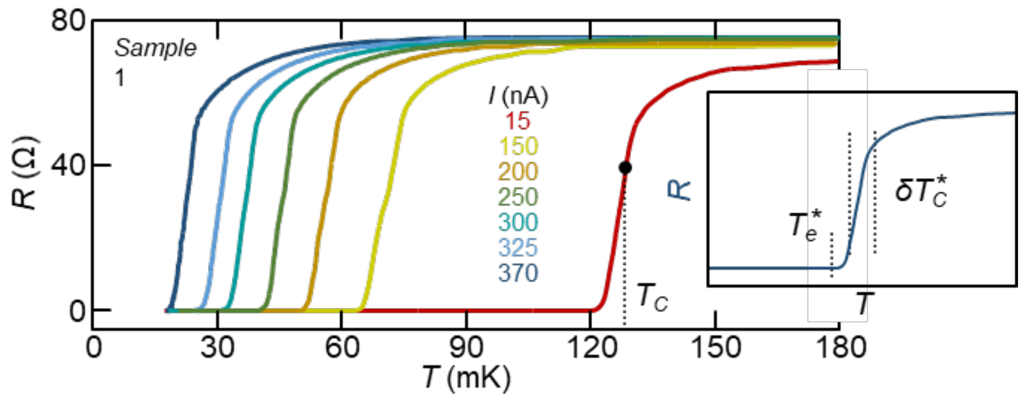

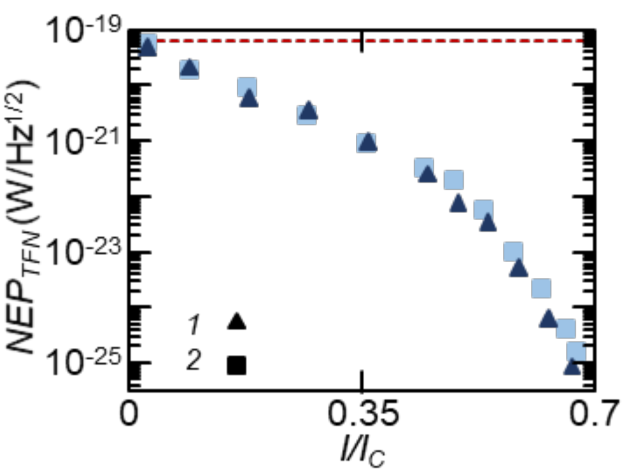

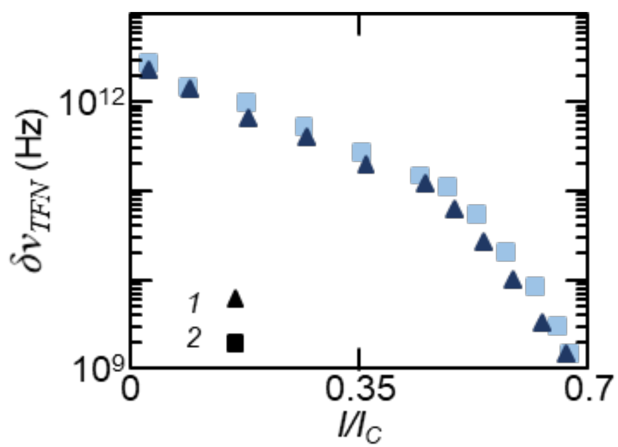

NEP:
$1x10^{-25}$ W/Hz$^{1/2}$

Frequency resolution:
2 GHz

Gyrotrons (often used for military-purpose/radar)

P(MW) x ν^2(GHz^2) = const.

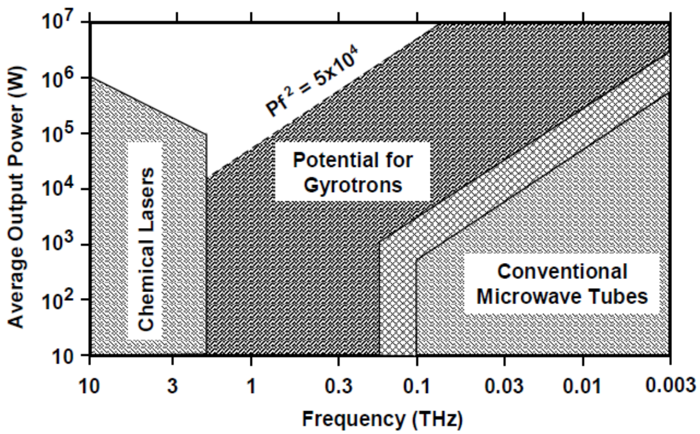

The operating region of gyrotrons

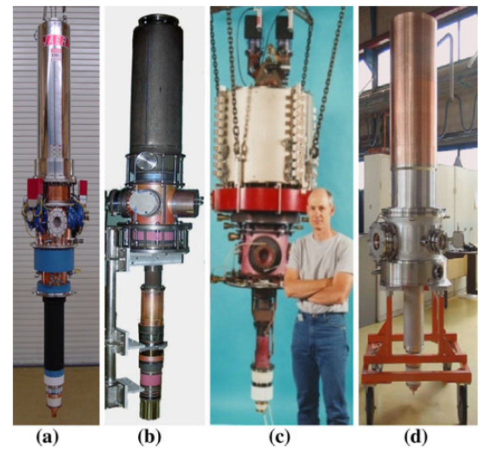

Fig. 2 Typical high power gyrotrons **a** JAERI/TOSHIBA 0.82 MW, 170 GHz, **b** GYCOM 1 MW, 170 GHz, **c** CPI 0.9 MW, 140 GHz, **d** TED 0.9 MW, 140 GHz

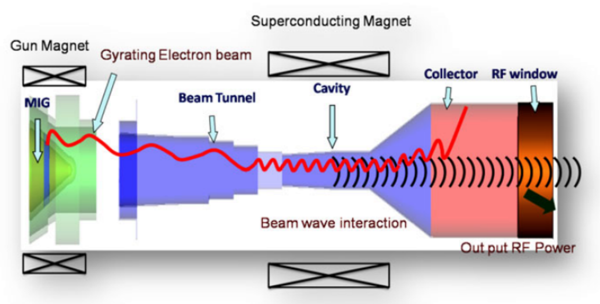

Now beyond 1 MW power

High-Power Cyclotron Autoresonance Maser (CARM)
Up to 10-15 MW with 10-50 GHz

Scheme of the temperatures in the experimental dilution cryostat set-up

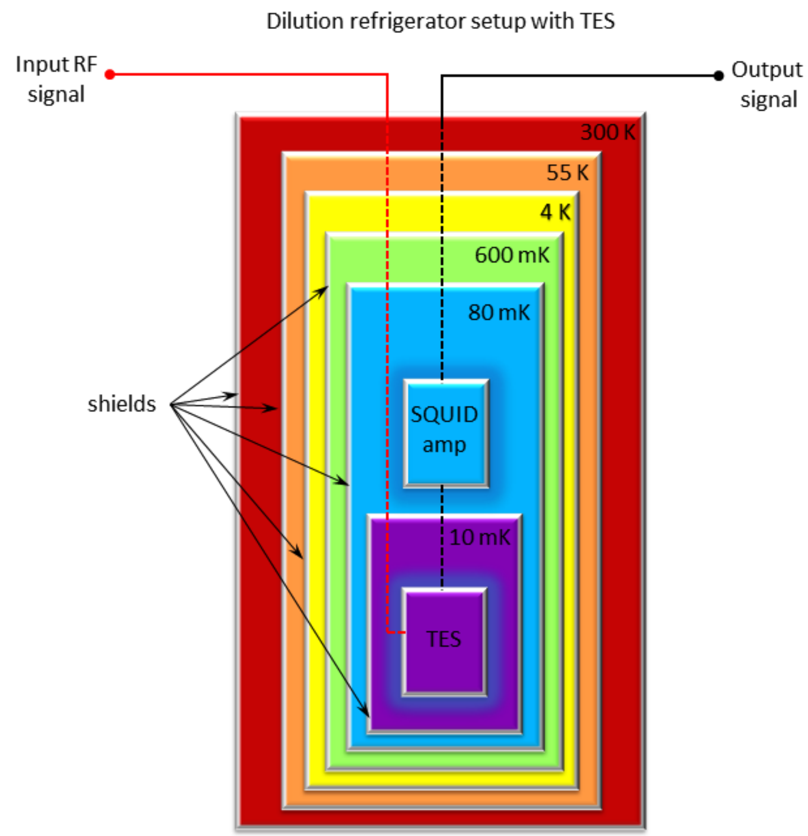

Figure 8 *Scheme of the experimental setup of the TES based on a dilution refrigerator. The cryostat metallic shields reside at different temperatures from 300 K to below ~ 10 mK. The enclosure containing the TES element is at the fridge base temperature whereas the readout SQUID amplifier is kept at 80 mK to improve its noise performance. Input microwave radiation is fed into the fridge, and thereby into the TES detector, via coaxial cables while the low-frequency output signal coming from the SQUID is read via conventional DC lines.*

STAX detector

- Tailoring TES active volume to reduce thermal capacitance **($V \sim 10^{-3}$-10^{-4} μm^3)**

$$\sigma_E \approx 0.3\sqrt{k_B T_c^2 C_e}$$

C = γ V T   V ~ 300x40x20 nm ^{3}

- low-noise SQUID readout electronics optimization (operating at 80 mK)
- Sensitivity $\delta T = \delta E / C_e$ thermalization $T(t) = \exp(-t/\tau)$ $\tau = C_e / G$

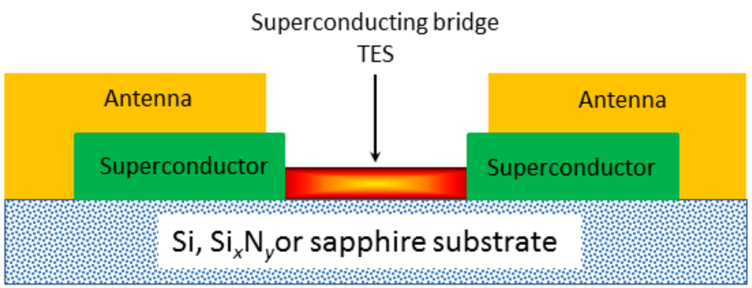

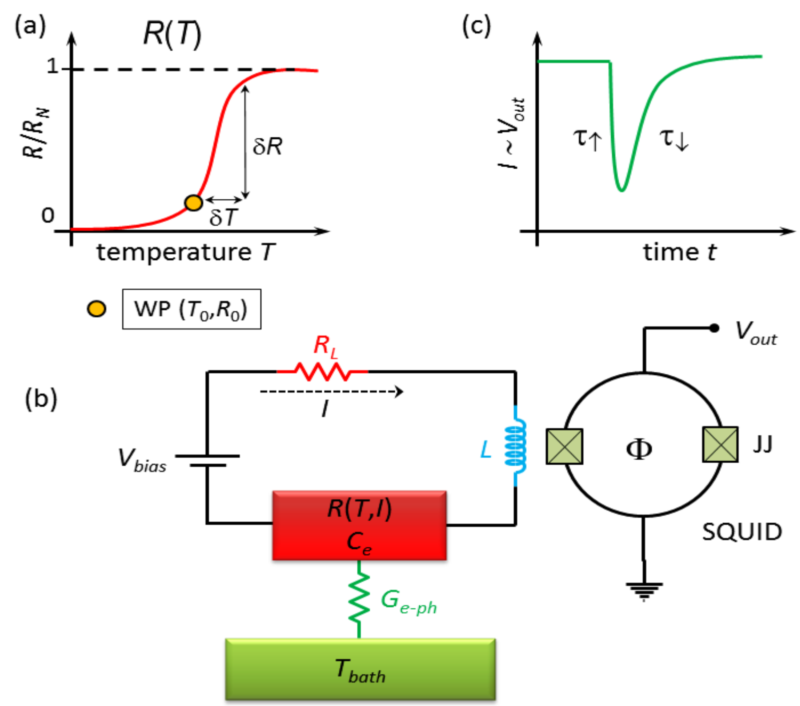

Noise

- Dark count rate (phonon noise) < 6×10^{-10} s^{-1}
- Black Body: at 10mK peaked around 0.6 GHz with a negligible rate of 10^{-30} m^{-2} s^{-1} photons irradiated
- Cosmic bkg: 1μ/cm^{-2}/min with 10 eV released in 10nm of material saturates the TES, bkg. under control translated in a negligible dead time of the TES ~ 0.1%

$$N_d = \frac{\beta_{eff}}{\sqrt{2\pi}} \int_{E_T/\sigma_E}^{\infty} exp(-x^2/2)\,\mathrm{d}x.$$

dark count bkg rate

where $\beta_{eff} = 1/\tau_{eff}$ is the effective detection bandwidth, and E_T is the discrimination threshold energy.

$$\eta = \frac{1}{\sqrt{2\pi}} \int_{(E_T - h\nu)/\sigma_E}^{\infty} exp(-x^2/2)\,\mathrm{d}x.$$

single photon quantum efficiency

Nano-fabrication: Shadow Mask Technique

Spin-coating with resist

E-beam lithography

Multiple evaporations

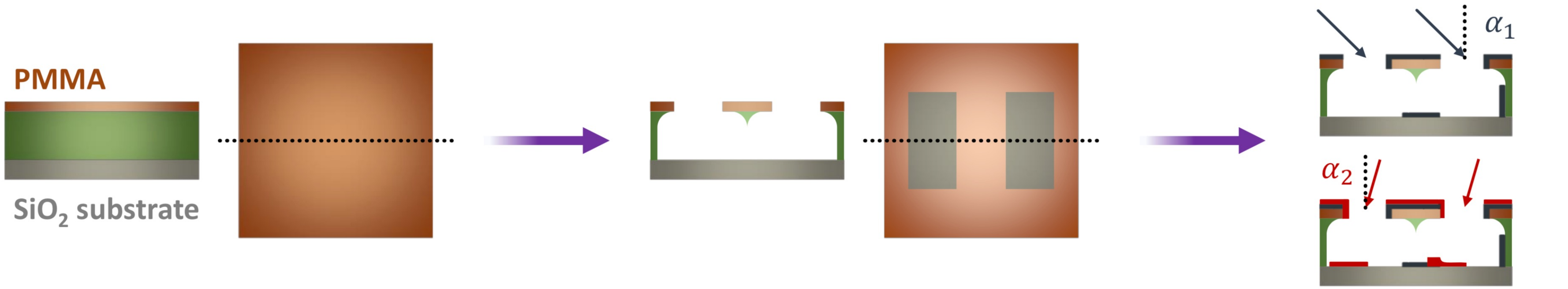

Final device

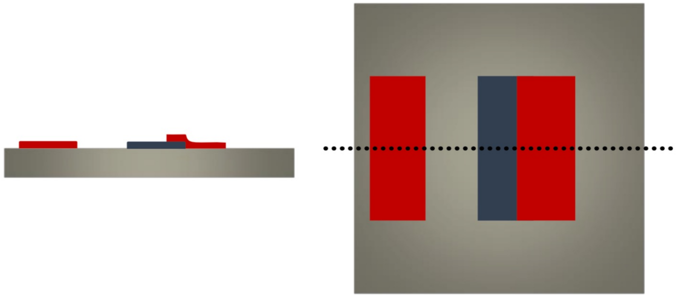

- Single lithography
- Single vacuum cycle
- High-quality metal-to metal contacts
- High quality metal-oxide interface

SIMP

- INFN LNF
- INFN PISA
- INFN SALERNO
- TIFPA
- INRIM
- CNR-NANO
- CNR-IFN

Nano-fabrication: Electron Beam Evaporation

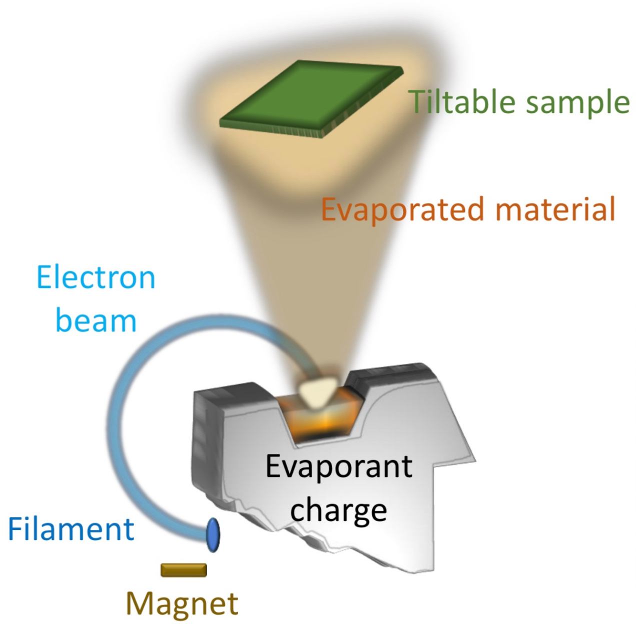

The deposition material undergoes the transition from solid to vapour state by means of electron bombardment

- Very low degree of contamination
- Deposition of uniform high-purity thin films
- Precise control of low or high deposition rates

Ultra-High Vacuum chamber

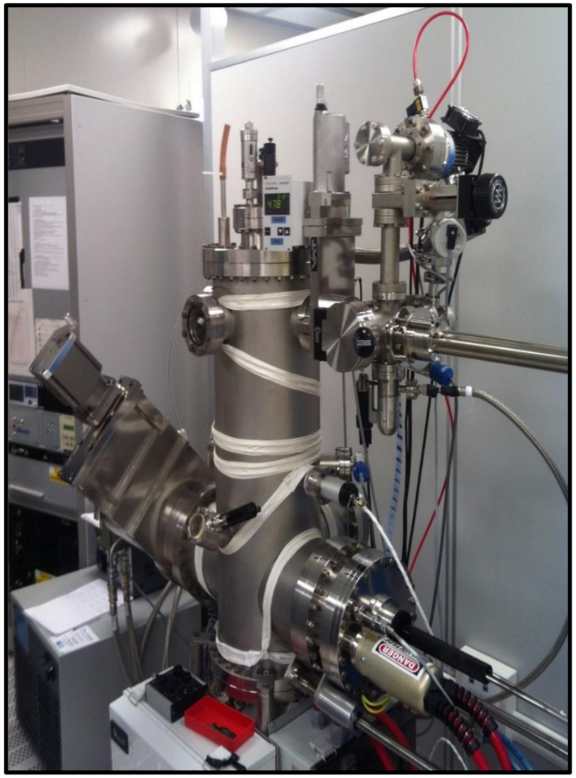

- Cu/Al and Cu/Ti bilayers designed as **5 μm X 200 nm strip** of different total thickness and thickness ratio

- Fabrication via e-beam lithography + e-beam evaporation

- 4-wires measurements of the resistance using a lock-in circuit

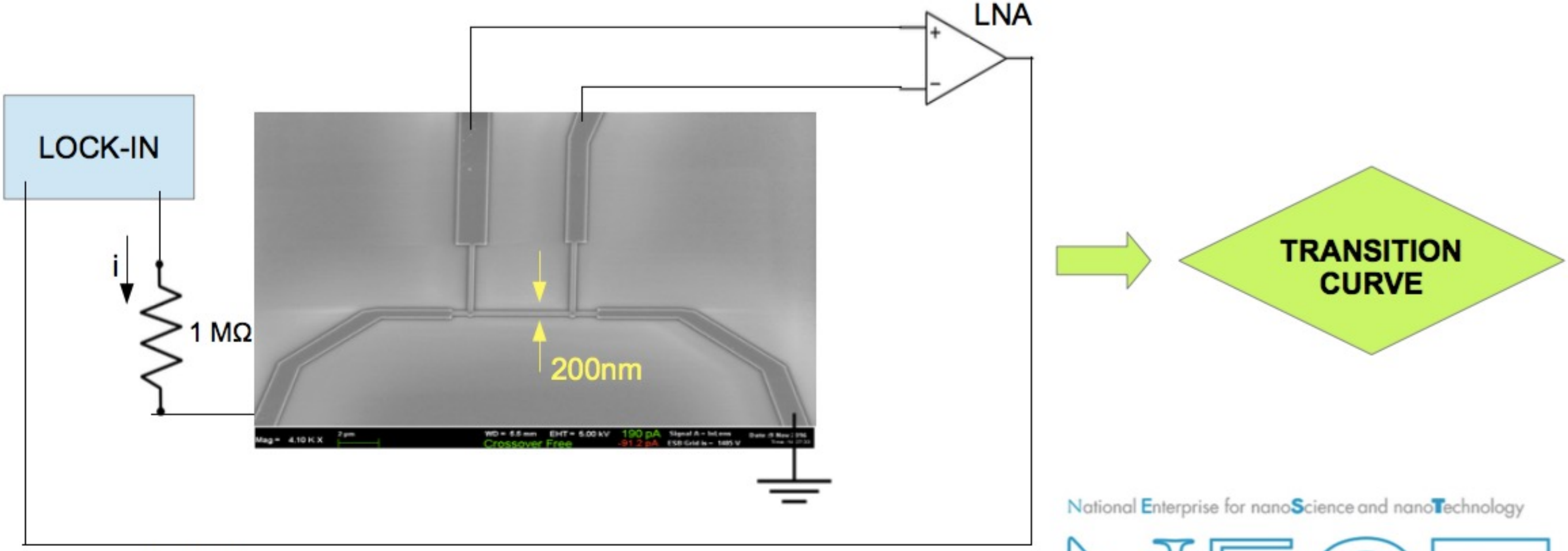

National Enterprise for nanoScience and nanoTechnology NEST

Yuri Venturini

Tc of Cu/Al bilayers (1)

all transitions are measured with a lock-in circuit with input current i = 6nA, except for Cu15Al10 (i=0.1nA)

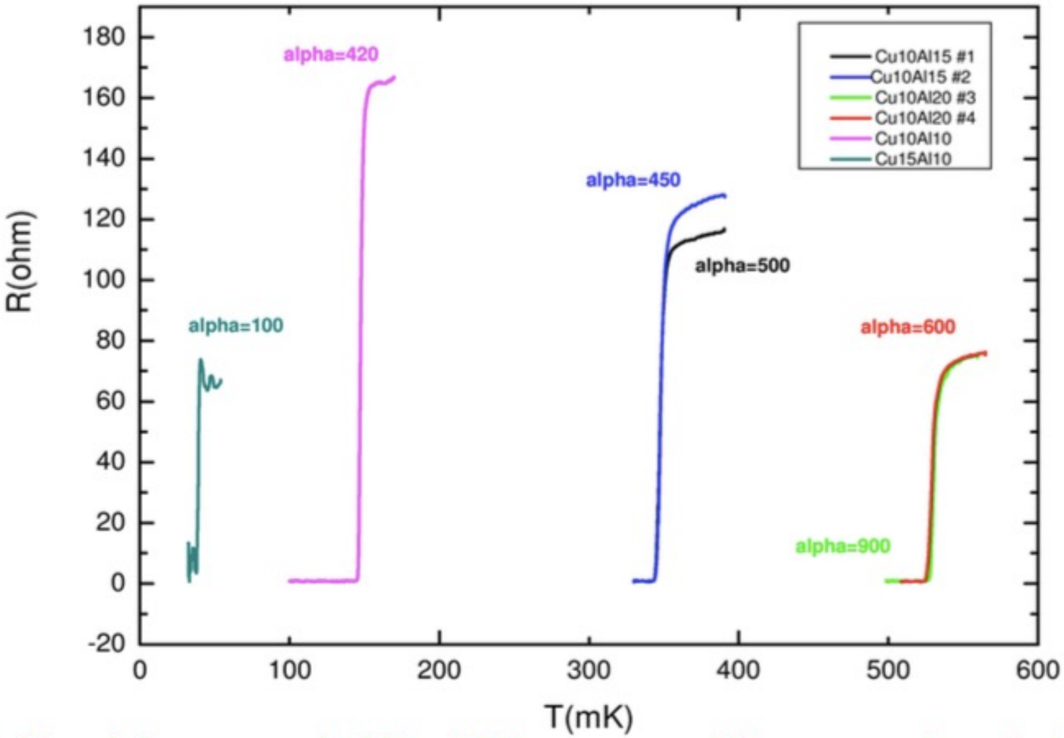

Data analysis: extraction of alpha=T/R * dR/dT

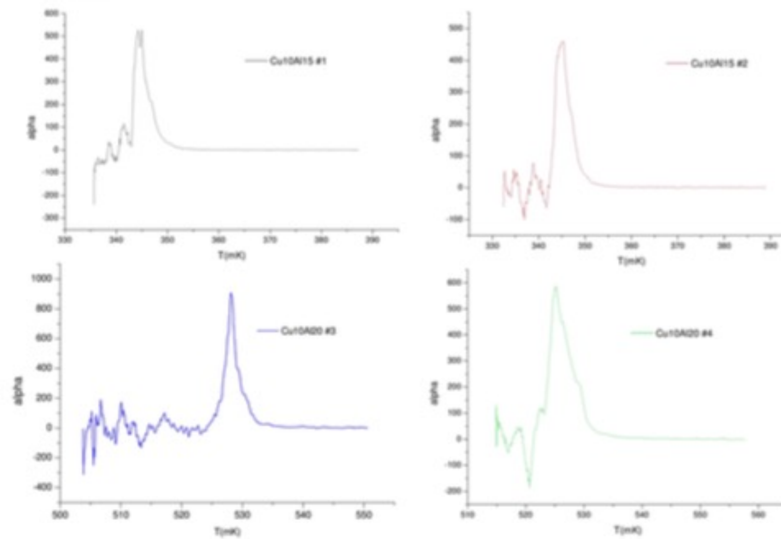

In the plot are reported the thicknesses and the max value of alpha

National Enterprise for nanoScience and nanoTechnology

Parameter	ALPS	STAX	g_{ALPS} / g_{STAX}	STAX II	g_{ALPS} / g_{STAXII}
Laser Power	0.8 W	100 kW	18.8	1 MW	188
Photon Energy	2.327 eV	124 µeV	11.7	124 µeV	11.7
Cavity Q-factor	55.0	10^4	3.7	10^8	37
$H * L_x$	22 T m	7.5 T m	0.3	7.5 T m	0.3
Detection Efficiency	0.9	1.0	1.0	1.0	1.0
Detector Noise	1.8 10^{-3} sec^{-1}	10^{-9} sec^{-1}	34.0	10^{-9} sec^{-1}	34
Combined Improvement			~ 10^4		~ $8x10^5$

Dark photons

L.B. Okun, Sov. Phys.-JETP **56**, 502 (1982)
B. Holdom, Phys. Lett. B **166**, 196 (1986)

- Massive vectors of hidden $U(1)_h$
- Visible and hidden-sector photons Lagrangian:

$$\mathcal{L} = -\frac{1}{4}F^{\mu\nu}F_{\mu\nu} - \frac{1}{4}B^{\mu\nu}B_{\mu\nu} + eJ^{\mu}_{\rm em}A_{\mu} + e_{\rm h}J^{\mu}_{\rm h}B_{\mu} - \frac{1}{2}\mu^2 B^{\mu}B_{\mu}$$

$F^{\mu\nu}$ = field strength tensor for A^{μ}; $B^{\mu\nu}$ = field strength tensor for B^{μ} (paraphoton)

- **A** and **B** rotated into $\mathbf{B}_1$ and $\mathbf{B}_2$; mixing angle $\chi < 10^{-2}$

$\mathbf{B}_1$ and $\mathbf{B}_2$ acquire masses $m_1 = \mu\chi$, $m_2 = \mu$

- Photon field evolve as:

$$A(r) = \frac{1}{\chi^2+1}e^{-i(\epsilon_\gamma t - k_1 r)}\left[A(1+\chi^2 e^{-iqr}) + \chi B(e^{-iqr} - 1)\right]$$

$$k_1 \approx \varepsilon_\gamma$$

$$k_2 \approx \sqrt{\varepsilon_\gamma^2 - \mu^2}$$

$$q = k_1 - k_2$$

Dark photons

L.B. Okun, Sov. Phys.-JETP **56**, 502 (1982)
B. Holdom, Phys. Lett. B **166**, 196 (1986)

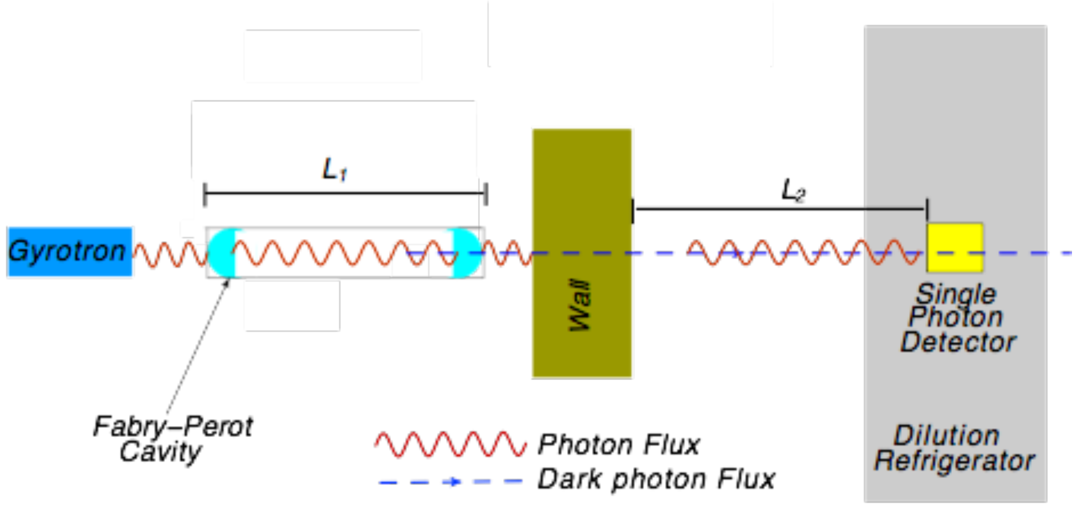

- Conversion probability: $P_{\gamma\to\gamma'}(r) = 4\chi^2 \sin^2\left(\frac{qr}{2}\right)$

$$P_{\gamma\to\gamma'\to\gamma} = P_{\gamma\to\gamma'}(L_1)P_{\gamma'\to\gamma}(L_2) = 16\chi^4\left[\sin\left(\frac{q\,L_1}{2}\right)\sin\left(\frac{q\,L_2}{2}\right)\right]^2$$

- Rate: $\frac{\mathrm{d}N_\gamma}{\mathrm{d}t} = \eta\,\Phi_\gamma\left[\frac{N_{\text{pass}}+1}{2}\right]P_{\gamma\to\gamma'\to\gamma}$

  Φ_γ = photon flux (s^{-1}), η = detector efficiency

Search for dark photons at STAX

L.M. Capparelli *et al.*, Phys. Dark Univ. **12**, 37 (2016)

- Exclusion limits STAX may achieve in case of null result

- **STAX** limits compared to
  - **ALPS LSW** results
    Phys. Lett. B **689**, 149 (2010)
  - **CROWS** results
    Phys. Rev. D **88**, 075014 (2013)
  - **Spring-8** results
    Phys. Lett. B **722**, 301 (2013)
  - **XENON10** results
    Phys. Lett. B **689**, 149 (2010)
  - Constraints on dark photons from measurements of the **CMB**
    Astrophys. J. **473**, 576 (1996)
  - Searches for modifications of **Coulomb's Law**
    Phys. Rev. Lett. **61**, 2285 (1988)